University of Birjand

Water Harvesting Research Vol. 7, No. 2, Autumn & Winter 2024, p. 246-257

10.22077/JWHR.2024.7445.1157

ORIGINAL ARTICLE

Assessment of Re-Forecast Data in the Modeling of Extreme Rainfall-Runoff Events (Case Study: Floods in the Bakhtiari Basin, Iran, March-April 2019)

Amin Eidipour[a], Mohammad Amin Maddah[a&*], Ali Mohammad Akhoond-Ali[a]

[a]Department of Hydrology and Water Resources, Faculty of Water and Environmental Engineering, Shahid Chamran University of Ahvaz, Ahvaz, Iran.

[*]Corresponding Author E-mail address: ma.maddah@scu.ac.ir

Received: 10 October 2024/ **Revised**: 11 November 2024/ **Accepted**: 23 November 2024

Abstract

Predicting inflow into reservoirs is essential for their operation during floods, particularly in mountainous watersheds characterized by snow-rain regimes. The objective of this research is to evaluate the GEFSv12 re-forecast data as an input of the HEC-HMS model for forecasting floods due to the extreme precipitation in March/April 2019 in the reservoir of Bakhtiari dam in southwestern Iran. So, ensemble flood forecasting (control and ensemble members) was conducted using extracted precipitation and temperature data with the lead-time up to 10 days. A sequence of predictions for flood warnings was analyzed when 50% of the members exceeded the threshold inflows of 1000 and 1500 m^3/s. The relative volume error values for the control member and the ensemble mean for five days ahead were -15% and -22%, respectively. While previous studies in catchments with snow-rain regimes anticipated challenges in flood forecasting at mid-lead times, this research demonstrated that the proposed probabilistic framework could effectively issue flood warnings for events with a lead time of five days. To address and predict flooding at the Bakhtiari Dam with a threshold of 1500 m^3/s, flood warnings are issued with a lead time of 5 to 8 days.

Keywords: Ensemble Forecasting, Flood Warning, GEFSv12, Hydrological Model, Reservoir Operation.

1. Introduction

Many meteorological centers around the world apply numerical weather prediction (NWP) models to produce precipitation forecasts. In some cases, the use of numerical weather and climate models inevitably leads to inaccurate prediction of runoff (Nanditha and Mishra, 2021). The important role of a reforecast in validating and calibrating weather and climate model forecasts, diagnosing model errors, and predicting extreme or rare events has therefore been widely recognized (Baxter et al., 2014; Ou et al., 2016; Gascón et al., 2019; Hamill et al. 2022).

Ensemble forecasting was developed to study and evaluate the efficiency of deterministic weather forecasting systems globally and locally. Ensemble forecasts are available in the re-forecast period and can be input directly into hydrologic models and used to assess the predictability of precipitation events, warn and guide farmers, and manage reservoirs (Stellingwerf et al., 2021). Over the past decade, ensemble flood forecasting has improved significantly with the development of numerical weather prediction models, advances in high-performance computing, and increasing interest in the transition from deterministic to probabilistic decision making (Wu et al., 2020). As for the probabilistic approach, ensemble forecasts consist of forecast elements that can be obtained from perturbations in the initial conditions of the weather and climate forecast model, hydrological models, and various numerical weather models (Moradkhani et al., 2018; Zhu et al., 2019).

An operational system that couples NWP and a hydrologic model at a basin scale was a practical strategy for predicting reservoir

inflow. Therefore, poor performance of the NWP model leads to errors in precipitation prediction, which in turn leads to uncertainties in runoff prediction (Fan et al., 2016; Nanditha and Mishra, 2021). Ensemble flood forecasts are usually based on ensemble forecasts based on different meteorological inputs, different initial conditions, multiple hydrological models, or a set of multiple parameters, or a combination of the above (Cloke and Pappenberger, 2009; Duan et al., 2019; Roundy et al., 2019).

The climate in Iran is generally dry and semi-arid, but frequent floods cause significant damage to people and society. A series of major floods occurred simultaneously in different parts of Iran in March/April 2019, causing massive damage to agriculture, farms, and residential areas (Aminyavari et al., 2019). In this context, Maddah et al. (2021) studied the extreme precipitation event of March-April 2019 in the Karkhe River basin in southwestern Iran. The results showed that the maximum and average values of rainfall predicted by the WRF model are underestimated and that the prediction error increases as the lead time increases. In general, they suggest that a forecast time of 78 to 102 hours is appropriate for warning of extreme precipitation events in the Karkhe River basin. Younis et al. (2008) studied the performance of the European Flood Alert System (EFAS) in part of the Elbe River basin in the Czech Republic for the 2006 spring precipitation event. The extreme flood event, triggered by snowmelt, caused major damage in the Elbe River basin. According to the analysis, EFAS forecasts were able to determine the flood probability signal 8 to 10 days in advance. In another study, Thielen et al. (2009) investigated the performance of the European Flood Alert System (EFAS) with a lead time of 3 to 10 days for international rivers in Europe.

Delaney et al. (2020) presented ensemble forecast operations (EFO) as a risk-based approach to reservoir flood control that includes ensemble streamflow predictions (ESPs) produced by the Nevada-California River Forecast Center. Reservoir operations are modeled separately for each of the ESP members to predict system conditions and calculate the risk of reaching critical operating thresholds. Decisions to release reservoirs for predicted risk management are simulated using the identified risk tolerance values. The EFO for Endocino Lake, California, is being developed to assess the extent to which it can improve reservoir storage reliability without increasing downstream flood risk.

Fan et al. (2016) used the GEFSv2 model from the United States National Oceanic and Atmospheric Administration. The researchers used a large-scale distributive hydrologic model from MGH-IPH, to produce an ensemble flood forecast for the Tocantins River basin in Brazil. The 2011/2012 precipitation season was simulated to forecast flood warnings for the reservoir and to examine ensemble members and flood lead time on a daily basis. Other researchers, such as Siqueira et al. (2020) and Wu et al. (2020), studied the importance of ensemble flood forecasts.

The literature search provided us with several studies on the use of re-forecast data and the production of runoff forecasts. However, there are fewer studies on evaluating and improving the forecasts in the watersheds of Iran. It was also found that in watersheds with dams, issuing flood warnings can play a greater role in reducing flood damage by pre-releasing from the reservoir ahead of time. Nevertheless, this should be investigated in different geographic areas.

This paper presents the results of ensemble flood forecasting based on GEFSv12 model for the extreme flood event in March and April 2019 in the Bakhtiari reservoir basin in southwestern Iran. In addition, the efficiency of using ensemble flood forecasts in the management of Bakhtiari reservoir was discussed.

2. Materials and Methods

In this section, first, Bakhtiari dam basin was introduced. Then, the method used in the rainfall-runoff conceptual model of HEC-HMS was described, followed by re-forecast precipitation and temperature input data of GEFSv12. Finally, the model evaluation indices were presented.

2.1. Study area

The study area was the Bakhtiari reservoir basin with an area of 6388 km^2 in southwestern Iran. Bakhtiari reservoir is located 80 km away

from Khoramabad city. Its main purpose is power generation and flood control (Hatamkhani et al., 2021). The maximum elevation above sea level of the basin is 4049 m. The Sezar and Bakhtiari rivers join about 3.1 km downstream of the dam to form the Dez River. The Great Karun is formed by the confluence of the Karun and Dez Rivers. The geographic location of the Bakhtiari dam is 48˚ 46’ 50” east longitude and 32˚ 57’ 41” north latitude. The Bakhtiari basin has a rain-snow regime. The average annual precipitation is about 720 mm, and the annual standard deviation of precipitation is 159.1 mm (Gheidari et al., 2011). Fig. 1 shows the topographic characteristics of the Bakhtiari reservoir basin and the locations of the meteorological stations.

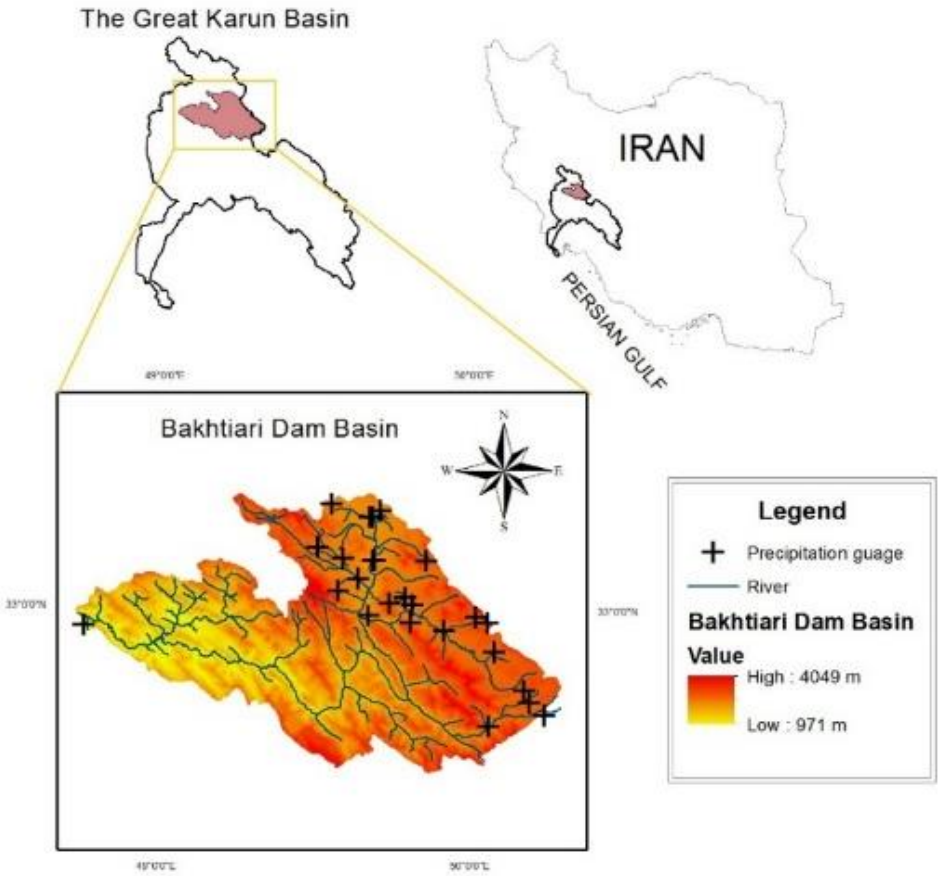

Fig. 1. Topographic properties of Bakhtiari dam basin and meteorological stations locations

2.2. Data collection

The Global Ensemble Forecasting System Version 12 (GEFSv12) data, recently launched, 31 years (1989-2019) of forecast data from the National Center for Environmental Prediction (NCEP) were used. The reforecast system is based on the NCEP global real-time forecast version 15.1 and uses the Finite Volume 3 dynamical core. The resolution of the forecast system is about 25 km with 64 vertical hybrid level and with a temporal resolution of 6 hours, i.e., available for 0, 6, 12, 18, and 24 hours (Guan et al., 2022). The newly forecast temperature and precipitation dataset GEFSv12 for the period 2000-2019 is available on the website https://noaa-gefs-retrospective.s3.amazonaws.com/index.html. The number of these forecasts outputs is not as much as that of the real-time forecasts. The initial conditions of the model are considered once per day according to the zero runtime. This model has five members, except that an 11-member reforecast is made once per week, and the lead time is 35 days. A critical aspect of the GEFS model is that these forecasts use a dynamic core where only the initial conditions are perturbed and there are some small random perturbations in the forecast phase. These forecasts are in contrast to systems such as the Short-Range Ensemble Forecast (SREF), where different dynamic cores are used in one set (Saminathan et al., 2021).

2.3. Model setup

In the present study, the soil moisture accounting (SMA) and snow melt algorithms (temperature index) available in HEC-HMS were used for continuous modeling of the rainfall-runoff process. According to Bennett (1998), the linear reservoir model was used along with the SMA model to calculate base flow, and the Clark model was used output of the models was used to convert excess precipitation to runoff (Teng et al., 2018).

HEC-HMS consists of three elements, including (1) the river basin model, (2) the meteorological model, and (3) the control specifications. Flowchart of the continuous modeling process undertaken in the present study using the HEC-HMS model is shown in Fig. 2. The snowmelt algorithm is a part of the meteorological model.

Snowmelt modeling is used to estimate snow water equivalent (SWE) volume and the timing and amount of snowmelt that affect soil moisture, runoff, and river flow. It is worth mentioning that the snowmelt algorithm (Temperature Index) is a key component of the meteorological model within the HEC-HMS. However, it is important to acknowledge the limitations of this model when applied to snow-affected basins with a rain-snow regime. For instance, the Temperature Index method relies on empirical temperature thresholds that may not accurately reflect local conditions, leading to potential inaccuracies in predicting snowmelt. Furthermore, the model does not account for complex interactions between precipitation forms, snowpack dynamics, and changing climatic conditions, which can impact the hydrological response (Gao et al., 2023; Houghton et al., 2022). These considerations highlight the need for careful application of the HEC-HMS model in snow-affected basins like the study area.

HEC-HMS provides two alternatives for modeling snowmelt, including (1) the temperature index method and (2) the gridded temperature index method (Davtalab et al. 2017). The river basin model is designed for modeling in two states (1) Continuous model (2) Event-based model.

Event-based flood modeling uses a simulation period of several hours to several days, beginning before precipitation and ending shortly after precipitation ends. Continuous modeling has longer time periods, including dry and wet periods, ranging from months to years (Gyawali and Watkins 2013). The Soil moisture accounting (SMA) algorithm pattern was introduced by Leavesley et al. (1983) and described by Bennett (1998). This model introduces the basin with a series of storage layers. Surface storage and tree canopy are the first layers to fill during precipitation. Surface infiltration then occurs. The third storage layer is then the soil profile storage. The water that exceeds the aforementioned storage appears as direct runoff. Evapotranspiration causes some of the water in the soil profile to be lost, and some of it reaches the groundwater layers via deep percolation. The calibrated parameters of the algorithm SMA are given in Table 1.

Table 1. Used values for parameters of the SMA model

Parameter	Calibrated value
Soil (%)	5
Groundwater 1(%)	20
Groundwater 2(%)	30
Max infiltration (mm/hr.)	2.41
Improvision (%)	0
Soil storage(mm)	945
Tension storage(mm)	669
Soil percolation (mm/hr.)	3.28
Gw 1 storage(mm)	220
Gw 1 percolation (mm/hr.)	1.59
Gw 1 coefficient(hr.)	1.35
Gw 2 storage(mm)	78.45
Gw 2 percolation (mm/hr.)	1.09
Gw 2 coefficient(hr.)	0.7

2.4. Evaluation criteria

The evaluation of the performance of the flood forecasting ensemble using the Nash-Sutcliffe efficiency (NSE), Pearson correlation coefficient (PCC), root mean square error (RMSE), and relative volume error (RVE) is presented in equations 1 to 4.

The NSE is often used to study the performance of hydrologic models. Nash and Sutcliffe (1970) defined a coefficient ranging from negative infinity to 1. Higher values indicate better efficiency. The NSE equation is:

$$NSE = 1 - \frac{\sum_{i=1}^{n}(o_i - p_i)^2}{\sum_{i-1}^{n}(o_i - \overline{p})^2} \quad (1)$$

PCC is a dimensionless index. It is the criteria for measuring the connection between

the changing trends for each corresponding paired variables. The PCC evaluates the similarity of variations in two variables (Kim et al., 2021). The PCC coefficient equals to:

$$PCC = \frac{\sum(O_i - \overline{O})\sum(P_i - \overline{p})}{\left[\sum(O_i - \overline{O})^2 \sum(P_i - \overline{P})^2\right]^{1/2}} \quad (2)$$

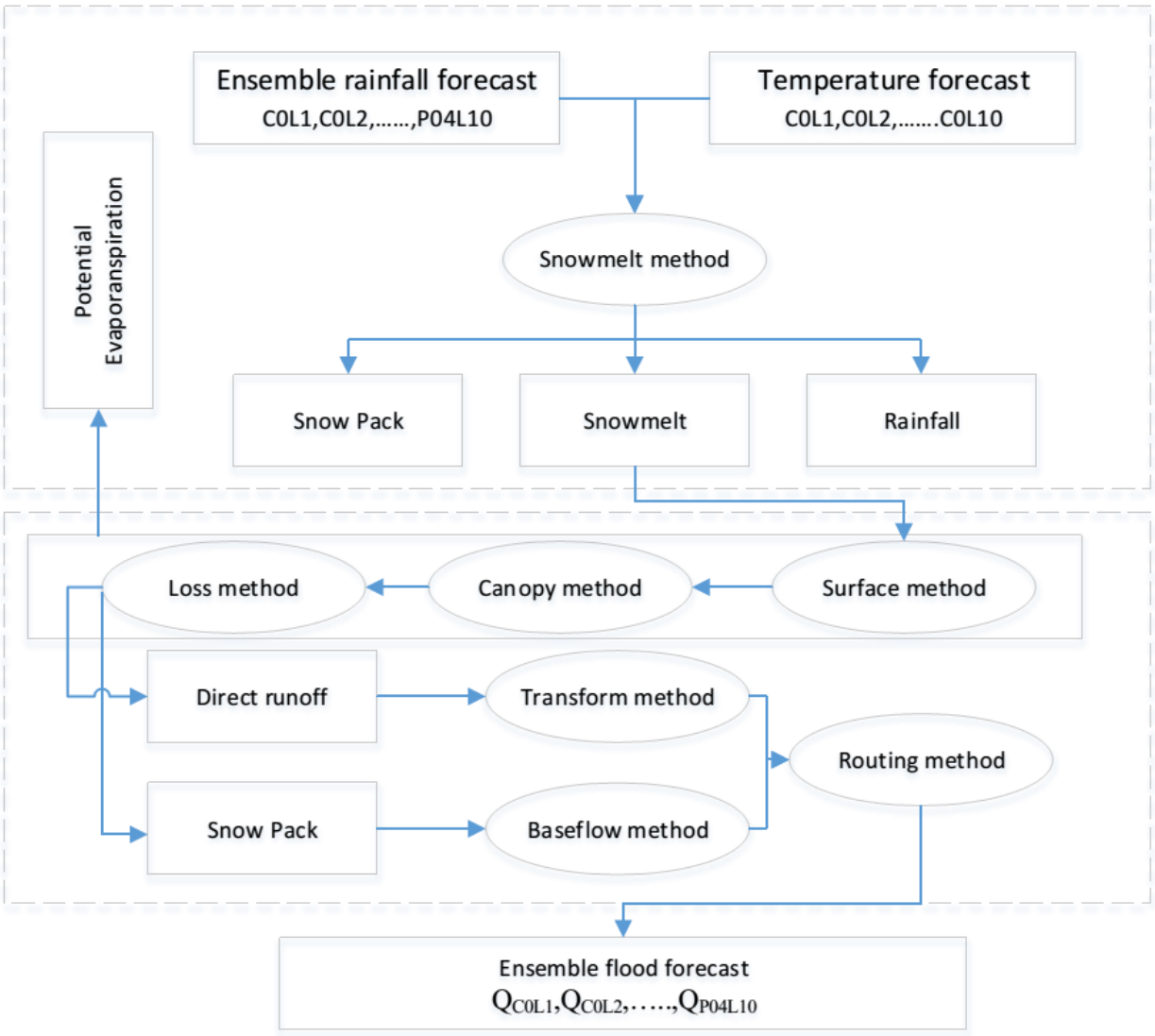

Fig. 2. Flowchart of the modeling process undertaken in the current study using the HEC-HMS model.

The RMSE is an index coaxial to the unit of measurement. The lower the RMSE value, the better the performance of the model. The RMSE can be significantly increased by a few large errors, which is the most critical problem with this test. In addition, the test does not distinguish between an underestimated and an overestimated value (Stone, 1993). RMSE is:

$$RMSE = \frac{1}{\overline{O}}\left[\frac{1}{n}\sum_{i=1}^{n}(P_i - O_i)^2\right]^{1/2} \quad (3)$$

The RVE percentage is used to compare the observed data volume with the simulated volume. This test shows whether the modeling is underestimating or overestimating. RVE equals:

$$RVE(\%) = \frac{\sum(O_i - P_i)}{\sum(O_i)} \times 100 \quad (4)$$

3. Results and Discussion

The efficiency of the continuous model HEC-HMS (SMA) for the Bakhtiari reservoir basin was evaluated using the index mentioned in section 2-4, and the results are reported here. The observed and simulated discharges during the calibration and evaluation periods are shown in Fig. 3.

SMA continuous model calibration was conducted over four years from 2015 to 2019, and the assessment was conducted over two years from 2019 to 2021. The NSE results for

the calibration and evaluation show values of 0.81 and 0.79, and the RMSE is 93 and 30, respectively (Table 2). Due to the large area of the catchment and the temporal and spatial variations in precipitation and snow storage and karst development in the study area, these criteria are a good indicator of model performance (Davtalab et al., 2017; Razmkhah et al., 2016). Although the model inputs are lumped, the model SMA was able to correctly simulate the physical processes of the watershed.

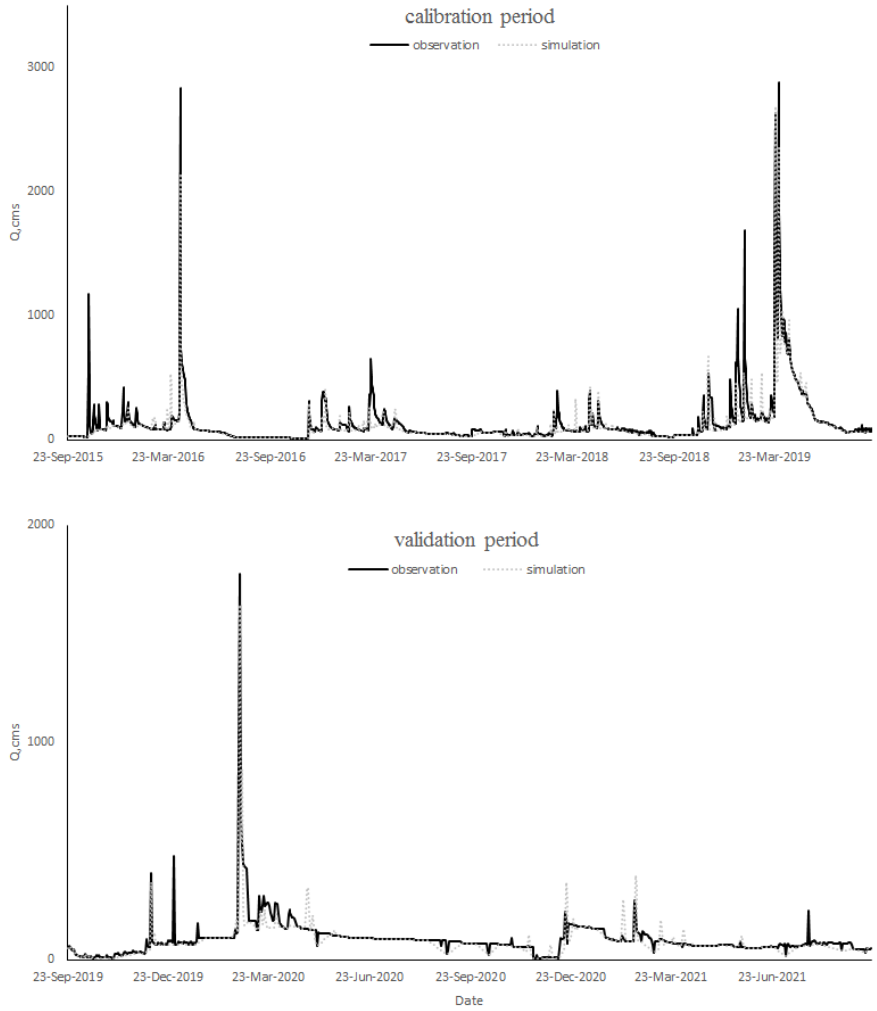

Fig. 3. Simulation and observation quantities of inflow (outflow) in the calibration (top) and evaluation (bottom) stage

Table 2. Results of the evaluation criteria of the model for the calibration and verification steps.

Criteria	Calibration	Verification
RVE (%)	-9	-7
NSE	0.81	0.79
RMSE (m^3/s)	93	30
PCC	0.91	0.90

The safe discharge range of the Dez River is between 1,000 and 1,500 m^3/s based on the river floodplain conditions and the current condition of the flood control structures downstream of the Dez Dam. Therefore, the lower limit of the no-damage discharge (1,000 m^3/s) and the minimum-damage discharge (1,500 m^3/s) were established as thresholds.

During the March-April 2019 study period, a precipitation event coinciding with snowmelt resulted in a severe flood with peak flows of 2600 and 2800 m^3/s. The flood lasted 13 days, with a daily discharge of 1500 m^3/s having been measured on 7 days. The physical conditions of the catchment and the considerable snow accumulation resulted in a slow decline of the hydrograph. Therefore, the flood generated 1570 million cubic meters of runoff. Fig. 4 shows the ensemble flood forecast results for 10 different lead times based on the GEFSv12 model members, including the control run, the four individual members, and the ensemble mean.

The heat map in Fig. 5 shows the results of NSE, RMSE, PCC, and RVE in 60 prediction sequences. Comparing the control run evaluation criteria values with those of the individual ensemble members and the ensemble mean, the better performance of the ensemble mean is evident.

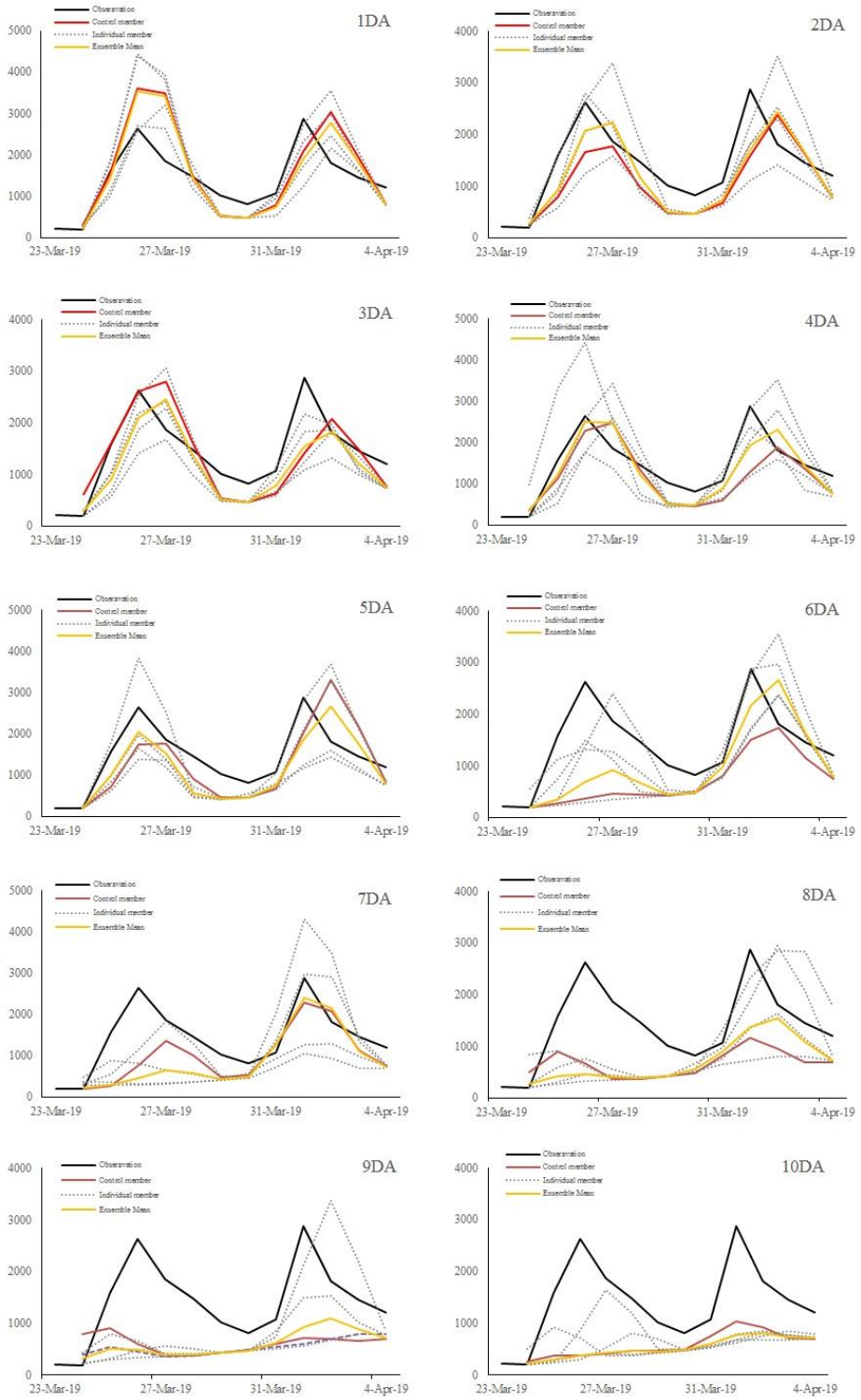

Fig. 4. Values of observed discharge and sequence of predictions for the March-April 2019 flood. Black lines illustrate the observed discharge. The x-axis represents time, while the y-axis shows discharge (m^3/s).

The criteria evaluation in the control run shows that 3 days ahead (3DA), the NSE, RMSE, PCC, and RVE values are 0.34, 540, 0.7, and -8, respectively, which is a better performance compared to the other lead times. However, the PCC is better for 1DA, its value is 0.79. The evaluation of each member of the ensemble shows that the indices tend to be

different for each member. The first and third individual members of 6DA had RVE index values of -14% and -4%, respectively, which were better than the control member's -52%. Examination of the ensemble mean shows that the NSE, RMSE, PCC, and RVE values for 4 days ahead (4DA) are 0.62, 442, 0.84, and -10, respectively, which is better than other lead times. However, the RVE value for 1DA has decreased to 6%. In general, the predicted volume is underestimated in most prediction sequences based on the RVE index. Nevertheless, 1DA is overestimated in all members except the fourth ensemble member. Accurate prediction of flood inflow is more critical to reservoir flood management than the shape and characteristics of the input hydrograph. Therefore, the RVE values show the model accuracy in predicting the inflow, which is more important for the operation of the reservoir.

Studies such as Block et al. (2009), Doblas-Reyes et al. (2005), and Gao et al. (2022) show better performance of the deterministic run compared to individual members. However, the results obtained for the study area showed that some individual members responded better than the control run. The results of the evaluation of the March-April 2019 flood criteria in the Bakhtiari reservoir basin showed that 2DA and 3DA performed better than 1DA for most indices. The results were in good agreement with studies such as Tsering et al. (2022) and Younis et al. (2008).

Members	Evaluated criteria	Days Ahead									
		1DA	2DA	3DA	4DA	5DA	6DA	7DA	8DA	9DA	10DA
Control member	NSE	-0.07	0.25	0.34	0.33	0.00	-1.06	-0.11	-1.10	-1.59	-1.48
	RMSE(cms)	737	617	580	583	713	1024	753	1034	1149	1124
	PCC	0.79	0.74	0.70	0.73	0.66	0.19	0.64	0.51	0.01	0.43
	RVE(%)	12	-25	-8	-19	-15	-52	-33	-55	-59	-61
EN(01)	NSE	0.20	-0.31	0.16	0.01	-0.12	0.22	-0.43	-1.07	-1.18	-1.86
	RMSE(cms)	639	818	655	710	755	628	853	1026	1054	1206
	PCC	0.81	0.57	0.72	0.57	0.78	0.70	0.62	0.26	0.43	0.31
	RVE(%)	6	-15	-28	-27	-41	-14	-43	-35	-55	-67
EN(02)	NSE	-0.56	0.58	0.14	-0.50	-0.19	0.03	-0.60	-1.32	-1.80	-1.62
	RMSE(cms)	893	462	663	874	777	702	903	1086	1193	1154
	PCC	0.81	0.84	0.71	0.72	0.82	0.71	0.64	0.65	0.14	0.23
	RVE(%)	20	-12	-28	11	13	-32	-46	-60	-64	-61
EN(03)	NSE	-0.61	0.43	0.50	0.03	0.03	-0.20	-1.07	-1.02	-0.99	-1.53
	RMSE(cms)	906	540	506	703	703	781	1027	1015	1006	1134
	PCC	0.75	0.78	0.81	0.71	0.69	0.58	0.45	0.27	0.40	0.34
	RVE(%)	12	-16	-8	-10	-16	-4	-34	-15	-29	-61
EN(04)	NSE	0.03	0.09	0.24	0.10	0.12	-1.14	-1.76	-1.24	-1.78	-1.05
	RMSE(cms)	701	775	621	676	764	1045	1185	1069	1190	1022
	PCC	0.66	0.91	0.83	0.74	0.98	0.28	0.48	0.38	0.30	0.40
	RVE(%)	-10	-16	-32	1	-41	-46	-19	-55	-65	-52
Ensemble mean	NSE	0.04	0.43	0.40	0.62	0.31	-0.42	-0.59	-1.05	-1.40	-1.74
	RMSE(cms)	701	537	551	442	594	851	900	1021	1105	1182
	PCC	0.78	0.78	0.79	0.84	0.77	0.55	0.54	0.43	0.44	0.35
	RVE(%)	6	-17	-21	-10	-22	-33	-40	-52	-60	-65

Lowest score — Highest score

Fig. 5. The heat map of the evaluation indices of prediction sequences

The ensemble members and the ensemble mean are critical in defining the probabilistic framework to make better decisions. By using an ensemble flood forecast, a dam's reservoir can be operated more efficiently during a flood, significantly reducing flood damage (Delaney et al., 2020). All lead times exceeding the thresholds of 1500 and 1000 m^3/s were examined using the probabilistic approach in Tables 3 and 4. If at least 50% of the members exceeded the thresholds, it was considered a serious flood warning (Fan et al., 2016).

The results from the probabilistic table for exceeding the threshold of 1500 m^3/s indicate a clear distinction in flood predictability between the two flood peaks. On March 26, during the first peak, there was no exceedance from 6DA to 10DA, while exceedance rates were significantly higher at earlier lead times (83% at 5DA and 100% at 4DA). This suggests that the early warning systems may need refinement for the first flood peak, as reliance

on the monitoring at 6DA and beyond did not indicate an imminent risk. In contrast, during the second peak on April 1, exceedance was detected as early as 7DA (67%), reaching 100% at 6DA, which demonstrates improved predictability and highlights the potential for better preparedness strategies during subsequent flood events. This finding aligns with previous research indicating that early-warning systems can significantly improve flood management by allowing responders to take timely action (García et al., 2017; Kousky, 2017).

Moreover, the results related to the threshold of 1000 m^3/s corroborate the efficacy of our warning systems, as alerts were issued prior to surpassing this critical level during both peaks. Notably, the higher percentage of exceedance (83%) for the second peak beginning at 8DA suggests that improved forecast accuracy may have contributed to earlier alerts, enhancing response effectiveness. This reinforces the notion discussed by Kousky (2017) that early warnings play a crucial role in flood risk management and community resilience. Overall, these findings emphasize the importance of continuous improvement in flood forecasting and warning mechanisms. Future studies could benefit from exploring advanced modeling techniques and integrating real-time data to further enhance the reliability of flood predictions.

Table 3. The exceedance of the flood threshold in March-April 2019, the numerical index corresponds to the percentage of ensemble members exceeding the discharge threshold of 1500 m^3/s (In the red area, the observed discharge is lower than 1500 m^3/s, and in the green area it is higher than 1500 m^3/s. The data marked with an asterisk shows the observed peak discharge).

lead time /date event	23	24	25	26*	27	28	29	30	31	1*	2	3	4
	March									April			
10DA	0	0	0	0	17	0	0	0	0	0	0	0	0
9DA	0	0	0	0	0	0	0	0	0	33	33	17	0
8DA	0	0	0	0	0	0	0	0	0	33	67	33	17
7DA	0	0	0	0	17	0	0	0	17	67	67	0	0
6DA	0	0	0	0	17	17	0	0	0	100	100	83	0
5DA	0	0	17	83	50	0	0	0	0	67	83	67	0
4DA	0	0	17	100	83	33	0	0	0	67	100	33	0
3DA	0	0	17	83	100	33	0	0	0	50	83	0	0
2DA	0	0	17	83	100	17	0	0	0	83	83	67	0
1DA	0	0	50	100	100	33	0	0	0	83	100	100	0

Table 4. Same as Table 3 but for 1000 m^3/s.

lead time /date event	23	24	25	26*	27	28	29	30	31	1*	2	3	4
	March									April			
10DA	0	0	0	0	17	17	0	0	0	17	0	0	0
9DA	0	0	0	0	0	0	0	0	0	33	50	33	0
8DA	0	0	0	0	0	0	0	0	17	83	67	67	17
7DA	0	0	0	17	33	33	0	0	67	100	83	67	0
6DA	0	0	17	50	50	17	0	0	33	100	100	100	0
5DA	0	0	17	100	100	0	0	0	17	100	100	100	0
4DA	0	0	50	100	100	67	0	0	33	100	100	83	0
3DA	0	0	50	100	100	83	0	0	17	100	100	83	0
2DA	0	0	17	100	100	67	0	0	0	100	100	100	0
1DA	0	0	83	100	100	100	0	0	17	100	100	100	0

4. Conclusion

The catchment area of the Bakhtiari reservoir is located in the high mountain zone of the Zagros Mountains in southwestern Iran. Consequently, extreme flood events are more likely to occur during the snowmelt season. The flood hydrograph in March-April 2019 shows that the second peak was larger than the first peak, although precipitation was higher at the same time as the first peak. Despite the complexity of the simulation process, especially in catchments with snow storage, the parametric uncertainty of the hydrological and meteorological model, the continuous model HEC-HMS (SMA) was able to correctly model the precipitation and runoff process. The generated ensemble flood forecast provides useful information for the Bakhtiari reservoir operator to improve flood management.

The performance of ensemble flood forecasts based on the GEFSv12 model was presented for the extreme event of March-April 2019. The results showed that although extreme events are always complicated, the use of probabilistic approaches is useful for decision making in flood management. With the proposed probabilistic framework, we could be notified 5-8 days before a flood event with discharge greater than 1500 m^3/s and 6-9 days before a flood with discharge greater than 1000 m^3/s. Although advance notification of reservoirs during this period has some limitations, especially if the floods occur at the end of the reservoir refilling period, it helps significantly in planning for preparedness and flood damage reduction.

5. Acknowledgment

We are very grateful to the research council of Shahid Chamran University of Ahvaz. and the Research Centre of Khuzestan Water and Power Authority.

6. Disclosure statement

No potential conflict of interest was reported by the authors.

7. References

Aminyavari, S., Saghafian, B., & Sharifi, E. (2019). Assessment of precipitation estimation from the NWP models and satellite products for the spring 2019 severe floods in Iran. *Remote Sensing, 11*(23), 2741.

Baxter, M. A., Lackmann, G. M., Mahoney, K. M., Workoff, T. E., & Hamill, T. M. (2014). Verification of quantitative precipitation reforecasts over the southeastern United States. *Weather and Forecasting, 29*(5), 1199–1207.

Bennett, T. (1998). Development and application of a continuous soil moisture accounting algorithm for the Hydrologic Engineering Center-Hydrologic Modeling System HEC-HMS. *University of California Davis.*

Block, P. J., Souza Filho, F. A., Sun, L., & Kwon, H. H. (2009). A streamflow forecasting framework using multiple climate and hydrological models 1. *JAWRA Journal of the American Water Resources Association, 45*(4), 828–843.

Cloke, H., & Pappenberger, F. (2009). Ensemble flood forecasting: A review. *Journal of Hydrology, 375*(3-4), 613–626.

Davtalab, R., Mirchi, A., Khatami, S., Gyawali, R., Massah, A., Farajzadeh, M., & Madani, K. (2017). Improving continuous hydrologic modeling of data-poor river basins using hydrologic engineering center's hydrologic modeling system: Case study of Karkheh River basin. *Journal of Hydrologic Engineering, 22*(8), 05017011.

Delaney, C. J., Hartman, R. K., Mendoza, J., Dettinger, M., Delle Monache, L., Jasperse, J., Ralph, F. M., Talbot, C., Brown, J., & Reynolds, D. (2020). Forecast informed reservoir operations using ensemble streamflow predictions for a multipurpose reservoir in Northern California. *Water Resources Research, 56*(9), e2019WR026604.

Doblas-Reyes, F. J., Hagedorn, R., & Palmer, T. (2005). The rationale behind the success of multi-model ensembles in seasonal forecasting—II Calibration and combination. *Tellus A: Dynamic Meteorology and Oceanography, 57*(3), 234–252.

Duan, Q., Pappenberger, F., Wood, A., Cloke, H. L., & Schaake, J. (2019). Handbook of hydrometeorological ensemble forecasting. Springer, Berlin/Heidelberg, Germany.

Fan, F. M., Collischonn, W., Quiroz, K., Sorribas, M., Buarque, D., & Siqueira, V. (2016). Flood forecasting on the Tocantins River using ensemble rainfall forecasts and real-time satellite rainfall estimates. *Journal of Flood Risk Management, 9*(3), 278–288.

Gao, L., Wei, J., Lei, X., Ma, M., Wang, L., Guan, X., & Lin, H. (2022). Simulation of an extreme precipitation event using ensemble-based WRF model in the southeastern coastal region of China. *Atmosphere, 13*(2), 194.

Gao, X., Zhang, X., & Wang, Y. (2023). Assessing the accuracy of snowmelt modeling in mountainous regions under climate change. *Hydrology Research, 54*(2), 120–135.

García, M., Martínez, A., & López, R. (2017). The role of early warning systems in disaster risk management. *International Journal of Disaster Risk Reduction, 21*, 46-54.

Gascón, E., Lavers, D., Hamill, T. M., Richardson, D. S., Ben Bouallègue, Z., Leutbecher, M., & Pappenberger, F. (2019). Statistical postprocessing of dual-resolution ensemble precipitation forecasts across Europe. *Quarterly Journal of the Royal Meteorological Society, 145*(724), 3218–3235.

Gheidari, M. H. N., Telvari, A., Babazadeh, H., & Manshouri, M. (2011). Estimating design probable maximum precipitation using multifractal methods and comparison with statistical and synoptic methods: Case study of

the Basin of Bakhtiari Dam. *Water Resources, 38*(4), 484–493.

Guan, H., Zhu, Y., Sinsky, E., Fu, B., Li, W., Zhou, X., Xue, X., Hou, D., Peng, J., & Nageswararao, M. (2022). GEFSv12 reforecast dataset for supporting subseasonal and hydrometeorological applications. *Monthly Weather Review, 150*(3), 647–665.

Gyawali, R., & Watkins, D. W. (2013). Continuous hydrologic modeling of snow-affected watersheds in the Great Lakes basin using HEC-HMS. *Journal of Hydrologic Engineering, 18*(1), 29–39.

Hamill, T. M., Whitaker, J. S., Shlyaeva, A., Bates, G., Fredrick, S., Pegion, P., Sinsky, E., Zhu, Y., Tallapragada, V., & Guan, H. (2022). The reanalysis for the Global Ensemble Forecast System Version 12. *Monthly Weather Review, 150*(1), 59–79.

Hatamkhani, A., Shourian, M., & Moridi, A. (2021). Optimal design and operation of a hydropower reservoir plant using a WEAP-based simulation–optimization approach. *Water Resources Management, 35*(5), 1637–1652.

Houghton, R. A., Jameson, A. K., & Clarke, D. (2022). Challenges in modeling snowmelt processes: A review of methodologies and their applicability to heterogeneous environments. *Journal of Hydrology, 608*, 127368.

Kim, S., Lee, J., Jeon, S., Lee, M., An, H., Jung, K., Kim, S., & Park, D. (2021). Correlation analysis between hydrologic flow metrics and benthic macroinvertebrates index (BMI) in the Han River Basin, South Korea. *Sustainability, 13*(20), 11477.

Kousky, C. (2017). Improving flood response through enhanced forecasting. *Water Resources Research, 53*(9), 7890-7903.

Leavesley, G., Lichty, R., Troutman, B., & Saindon, L. (1983). Precipitation-runoff modeling system: User's manual. *Water-Resources Investigations Report 83*:4238.

Maddah, M. A., Akhoond-Ali, A. M., Ahmadi, F., Ghafarian, P., & Rusin, I. N. (2021). Forecastability of a heavy precipitation event at different lead times using WRF model: The case study in Karkheh River basin. *Acta Geophysica, 69*(5), 1979–1995.

Moradkhani, H., Nearing, G., Abbaszadeh, P., & Pathiraja, S. (2018). Fundamentals of data assimilation and theoretical advances. In Handbook of hydrometeorological ensemble forecasting (pp. 1–26).

Nanditha, J., & Mishra, V. (2021). On the need for ensemble flood forecasting in India. *Water Security, 12*, 100086.

Nash, J. E., & Sutcliffe, J. V. (1970). River flow forecasting through conceptual models part I—A discussion of principles. *Journal of Hydrology, 10*(3), 282–290.

Ou, M. H., Charles, M., & Collins, D. C. (2016). Sensitivity of calibrated week-2 probabilistic forecast skill to reforecast sampling of the NCEP Global Ensemble Forecast System. *Weather and Forecasting, 31*(4), 1093–1107.

Razmkhah, H., Saghafian, B., Akhoond-Ali, A. M., & Radmanesh, F. (2016). Rainfall-runoff modeling considering soil moisture accounting algorithm: Case study of Karoon III River basin. *Water Resources, 43*(4), 699–710.

Roundy, J. K., Duan, Q., & Schaake, J. C. (2019). Handbook of hydrometeorological ensemble forecasting (pp. 3–31).

Saminathan, S., Medina, H., Mitra, S., & Tian, D. (2021). Improving short to medium range GEFS precipitation forecast in India. *Journal of Hydrology, 598*, 126431.

Siqueira, V. A., Fan, F. M., De Paiva, R. C. D., Ramos, M. H., & Collischonn, W. (2020). Potential skill of continental-scale medium-range ensemble streamflow forecasts for flood prediction in South America. *Journal of Hydrology, 590*, 125430.

Stellingwerf, S., Riddle, E., Hopson, T. M., Knievel, J. C., Brown, B., & Gebremichael, M. (2021). Optimizing precipitation forecasts for hydrological catchments in Ethiopia using statistical bias correction and multi-modeling. *Earth and Space Science, 8*(6), e2019EA000933.

Stone, R. (1993). Improved statistical procedure for the evaluation of solar radiation estimation models. *Solar Energy, 51*(4), 289–291.

Teng, F., Huang, W., & Ginis, I. (2018). Hydrological modeling of storm runoff and snowmelt in Taunton River Basin by applications of HEC-HMS and PRMS models. *Natural Hazards, 91*(1), 179–199.

Thielen, J., Bartholmes, J., Ramos, M. H., & De Roo, A. (2009). The European flood alert system–part 1: Concept and development. *Hydrology and Earth System Sciences, 13*(2), 125–140.

Tsering, K., Shrestha, M., Shakya, K., Bajracharya, B., Matin, M., Lozano, J. L. S., Nelson, J., Wangchuk, T., Parajuli, B., & Bhuyan, M. A. (2022). Verification of two hydrological models for real-time flood forecasting in the Hindu Kush Himalaya (HKH) region. *Natural Hazards, 110*(3), 1821–1845.

Wu, W., Emerton, R., Duan, Q., Wood, A. W., Wetterhall, F., & Robertson, D. E. (2020).

Ensemble flood forecasting: Current status and future opportunities. Wiley Interdisciplinary Reviews: *Water, 7*(3), e1432.

Younis, J., Ramos, M. H., & Thielen, J. (2008). EFAS forecasts for the March–April 2006 flood in the Czech part of the Elbe River Basin—A case study. *Atmospheric Science Letters, 9*(2), 88–94.

Zhu, Y., Li, W., & Sinsky, E. (2019). An investigation of prediction and predictability of NCEP Global Ensemble Forecast System (GEFS).